EXTENSION OF THE OPERATING POINT OF THE MERCURY IVA FROM 6 TO 8 MV*

R. J. Allen[ξ], R. J. Commisso, G. Cooperstein[a], P. F. Ottinger[a] and J. W. Schumer

Plasma Physics Division
Naval Research Laboratory
Washington, DC 20375 USA

Abstract

The output voltage of the NRL Mercury generator has been successfully increased to 8 MV. Mercury was originally designed for 6 MV, 300 kA operation in negative polarity [1]. However, new experiments required a bremsstrahlung x-ray source with a higher endpoint voltage [2],[3]. The threshold energy for photofission in targets of interest is about 5.5 MeV and, given the roughly Gaussian shape of the Mercury output pulse, very few x rays above threshold could be generated by Mercury with a 6-MV peak output voltage. Also, the cross section for fission rises sharply above the threshold energy. It was therefore decided to increase the output voltage of Mercury to the maximum possible without imposing undo cost or risk. A new center conductor was designed for Mercury that increased the effective output impedance of the MITL from about 23 to 40 Ω, thereby increasing the maximum output voltage to 8 MV. The new center conductor has carefully designed tapers (steps down in diameter) at each stage of the adder so that the adder cell voltages are equally balanced at the design limit of 1.3 MV. One limiting factor is the breakdown probability of the insulator stack in the adder cells. However, simulations have shown that the new center conductor only increases the breakdown probability a small amount. The 40 Ω output impedance was selected because it allowed us to reuse several pieces of the existing center conductor. Aluminum was used for most of the new parts. These steps allowed us to save time and keep material costs to a minimum. PIC and circuit simulations were performed to validate the design. Mercury has now been successfully operated for over 200 shots at 8 MV.

I. INTRODUCTION

The original design of the Mercury IVA allowed operation at 6 MV and 300 kA [1]. Although the center conductor was designed in a way more suited for positive polarity, it also functioned well in negative polarity [4]. However, new programs involving active detection of fissile materials required increasing the output voltage of Mercury to at least 8 MV. The reason for this is shown in a very simplistic way in Figure 1. This figure shows idealized bremsstrahlung spectra at 6 and 8 MV output voltage (green and blue lines, respectively) along with a sketch of a photo-fission yield curve for a fissionable material (red curve) that has a threshold ~5.5 MV and then increases superlinearly out to 8 MV.

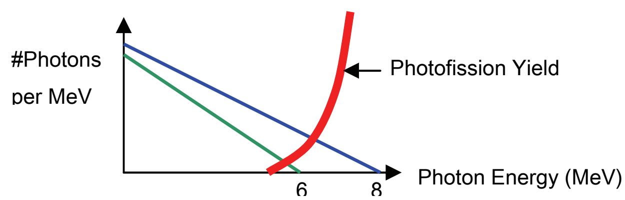

Figure 1. Idealized bremsstrahlung spectra at 6 (green) and 8 MV (blue) output voltage along with a sketch of a photofission yield curve (red).

The number of photofissions produced at 6 or 8 MV peak output voltage is calculated by integrating the product of the bremsstrahlung spectrum and the photofission yield curve. It is believed that the overlap between the 6 MV bremsstrahlung and yield curves is insufficient for IPAD (Intense Pulsed Active Detection) experiments [4],[5], especially given the approximately Gaussian output pulse shape that only exceeds 5.5 MV for a short time. With the extension of the operating point of Mercury to 8 MV, we obtain significant overlap and therefore orders of magnitude more photofissions per shot.

As an additional benefit of the change to 8 MV, even though the output current of Mercury is reduced from 300 to 200 kA (explained later), the bremsstrahlung dose rate output is still expected to increase significantly. This will be useful for other programs such as weapon effects and radiography.

[*] Work supported by ONR

[ξ] email: allen@nrl.navy.mil
[a] L3 Communications, Inc, Reston, VA.

Report Documentation Page

Form Approved
OMB No. 0704-0188

1. REPORT DATE	2. REPORT TYPE	3. DATES COVERED
JUN 2011	**N/A**	**-**

4. TITLE AND SUBTITLE
Extension Of The Operating Point Of The Mercury Iva From 6 To 8 Mv

5a. CONTRACT NUMBER

5b. GRANT NUMBER

5c. PROGRAM ELEMENT NUMBER

6. AUTHOR(S)

5d. PROJECT NUMBER

5e. TASK NUMBER

5f. WORK UNIT NUMBER

7. PERFORMING ORGANIZATION NAME(S) AND ADDRESS(ES)
Plasma Physics Division Naval Research Laboratory Washington, DC 20375 USA

8. PERFORMING ORGANIZATION REPORT NUMBER

9. SPONSORING/MONITORING AGENCY NAME(S) AND ADDRESS(ES)

10. SPONSOR/MONITOR'S ACRONYM(S)

11. SPONSOR/MONITOR'S REPORT NUMBER(S)

12. DISTRIBUTION/AVAILABILITY STATEMENT
Approved for public release, distribution unlimited

13. SUPPLEMENTARY NOTES
See also ADM002371. 2013 IEEE Pulsed Power Conference, Digest of Technical Papers 1976-2013, and Abstracts of the 2013 IEEE International Conference on Plasma Science. IEEE International Pulsed Power Conference (19th). Held in San Francisco, CA on 16-21 June 2013., The original document contains color images.

14. ABSTRACT
The output voltage of the NRL Mercury generator has been successfully increased to 8 MV. Mercury was originally designed for 6 MV, 300 kA operation in negative polarity [1]. However, new experiments required a bremsstrahlung x-ray source with a higher endpoint voltage [2],[3]. The threshold energy for photofission in targets of interest is about 5.5 MeV and, given the roughly Gaussian shape of the Mercury output pulse, very few x rays above threshold could be generated by Mercury with a 6-MV peak output voltage. Also, the cross section for fission rises sharply above the threshold energy. It was therefore decided to increase the output voltage of Mercury to the maximum possible without imposing undo cost or risk. A new center conductor was designed for Mercury that increased the effective output impedance of the MITL from about 23 to 40 Ù, thereby increasing the maximum output voltage to 8 MV. The new center conductor has carefully designed tapers (steps down in diameter) at each stage of the adder so that the adder cell voltages are equally balanced at the design limit of 1.3 MV. One limiting factor is the breakdown probability of the insulator stack in the adder cells. However, simulations have shown that the new center conductor only increases the breakdown probability a small amount. The 40 Ù output impedance was selected because it allowed us to reuse several pieces of the existing center conductor. Aluminum was used for most of the new parts. These steps allowed us to save time and keep material costs to a minimum. PIC and circuit simulations were performed to validate the design. Mercury has now been successfully operated for over 200 shots at 8 MV.

15. SUBJECT TERMS

16. SECURITY CLASSIFICATION OF:			17. LIMITATION OF ABSTRACT	18. NUMBER OF PAGES	19a. NAME OF RESPONSIBLE PERSON
a. REPORT **unclassified**	b. ABSTRACT **unclassified**	c. THIS PAGE **unclassified**	**SAR**	**6**	

II. MERCURY CIRCUIT MODEL AND SELF-LIMIT OF MITL

A simple circuit model of Mercury is given by using the Thevenin equivalent of it's PFL outputs into the IVA, under the assumption that the IVA is working perfectly. The PFL output lines, after the prepulse/sharping water switch have 6.78-Ω impedance. With the normal operating conditions of Mercury, including a 75-kV Marx charge voltage, the forward going waves from the PFLs have a 1.0 MV pulse height. With all of the six IVA cells in series, each fed by two PFLs in parallel, the Thevenin equivalent is a 12-MV source voltage with a 20.34-Ω source impedance as shown in Fig. 2.

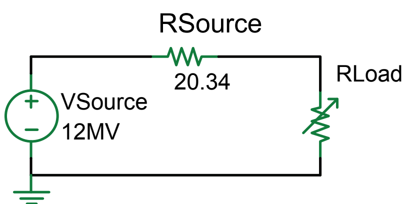

Figure 2. A simple Thevenin equivalent circuit model of Mercury based on PFL output impedance and voltage.

This simple circuit model can be used to generate a load line, which defines the load voltage and current with a variable load resistance, as shown by the black line in the graph of Fig. 3. This load line shows that one way to increase the load voltage is to increase the load resistance, at the expense of load current. However, the output of Mercury is an MITL (magnetically-insulated transmission line) which has a self-limited impedance that can be calculated given it's vacuum impedance of 30 Ω. This self-limited impedance (shown as the blue curve in Fig. 3) with the original center conductor of Mercury can be approximated as a constant 24-Ω impedance limit that cannot be exceeded.

Another way to increase the load voltage is to increase the Marx charge voltage. This moves the load line outward outward and increases both load voltage and current at the self-limited point. In fact, Mercury has been operated many times in the past with a 78-kV Marx charge and widened PFL water switch gaps to produce 1.1 MV forward going waves and approximately 7 MV into a self-limited load. However, this already increased the intermediate-store capacitors, laser switches, and PFL components to higher than designed values. Because of the expense and down time required to repair failures in these components, it was decided to replace the center conductor in the Mercury IVA with a narrower version. The new narrower center conductor increases the self-limited impedance of the MITL output of Mercury, allowing us to reach 8 MV with a 75-kV Marx charge voltage.

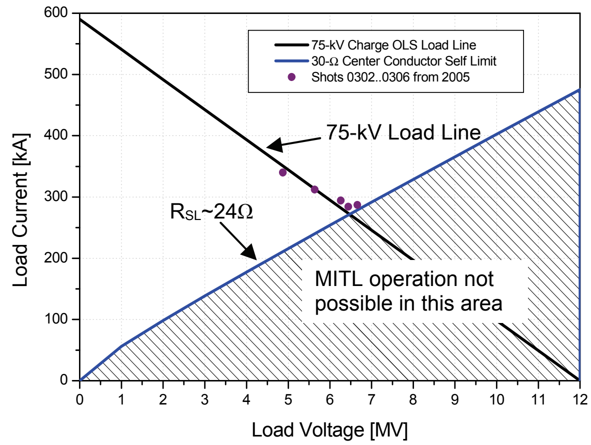

Figure 3. The load line of Mercury from it's simple Thevenin equivalent, the self limit curve from the original, 30-Ω center conductor and actual data from Mercury shots with different load impedances.

From the load line, it is clear that the new center conductor needs a 40-Ω self-limited impedance to reach 8 MV with 75-kV Marx charge voltage. The extended operating range of Mercury with the new, 49-Ω vacuum impedance, center conductor is shown in Fig. 4, where the new self-limited point is 8 MV and 200 kA. Fig. 4 also shows that the same 6 MV at 300 kA output could still be achieved with the new center conductor by reducing the load impedance. Note that for some applications, this would be preferable to the previous self-limited 6 MV operating mode since it can be shown that less of the 300 kA current would be in electron flow [6]. However, for active detection, only operating at the self-limited point is currently being considered.

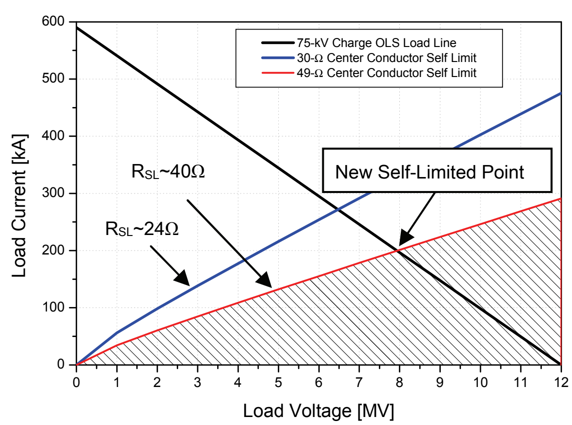

Figure 4. The Mercury 75-kV charge load line with the new self-limited curve given by a new center conductor with vacuum impedance increase from 30 to 49 Ω to give a 40-Ω self-limited impedance at 8 MV.

III. CENTER CONDUCTOR DESIGN

The new center conductor for Mercury was designed to have a 40-Ω self-limited impedance at the output end to give the desired 8 MV, 200 kA operating point. But, the center conductor needs to change diameter as it threads the IVA cells. This is required in order for the adder to function properly and to equalize cell voltages [7].

A. Ideal Center Conductor Design

The IVA can be viewed as a transmission-line voltage adder as shown in Fig. 5a, ignoring the need for magnetic cores to keep the outer surface of the machine at ground potential. The parallel combination of two PFLs that feed each of the six stages of the transmission-line voltage adder give a forward going wave voltage, V_S = 1.0 MV, with a source impedance, Z_S = 3.38 Ω.

The transmission-line voltage adder works perfectly under the condition that

$$Z_N = \left(\frac{N}{6}\right) R_L \tag{1}$$

so as to have equal steps in impedance down the adder. In this case, the circuit can be shown by circuit analysis to be equivalent to that of Fig. 5b where a forward going wave of $6*V_S$ = 6.0 MV feeds a transmission line with impedance of $6*Z_S$ = 20.34 Ω that drives the load. This circuit can be further simplified to that of Fig. 5c, which is identical to the Thevenin equivalent circuit shown in Fig. 2 where the source term equals twice the forward going wave voltage.

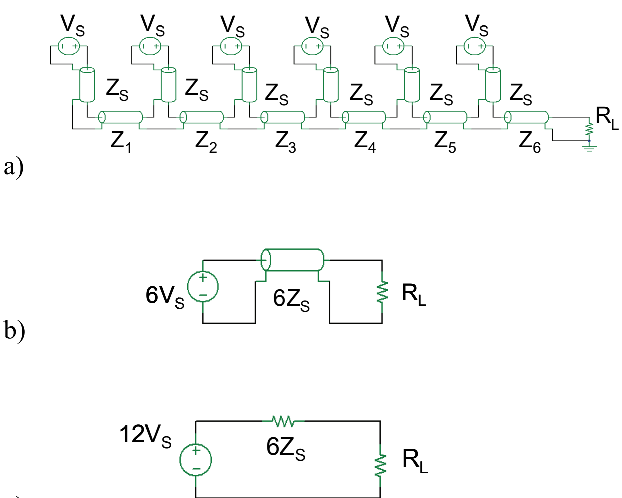

Figure 5. Circuit diagram of a transmission-line voltage adder (a), a simplified, equivalent circuit under condition of equal impedance steps (b), and further simplification to Thevenin equivalent circuit (c).

With the intent to operate Mercury at 8 MV with 75-kV Marx charge, this transmission-line voltage adder circuit model shows that the ideal center conductor has six equal 6.7 Ω steps in self-limited impedance ending with a 40-Ω section matching the self-limited load impedance.

B. MITL Theories for Center Conductor Diameters

From the previous section, the ideal impedance and voltage in each of the 6 MITL sections of the IVA is shown in Fig. 6 atop of a LSP PIC (particle-in-cell) code [8] 2D simulation particle plot of the Mercury adder with these parameters. In that simulation, the load is forced to be self-limited by suppressing electron emission at the end of the center conductor. Although LSP could be used to determine the required center conductor diameter in each section, it would be a time consuming process and so analytical MITL theory was used to determine the required diameter in each section of center conductor.

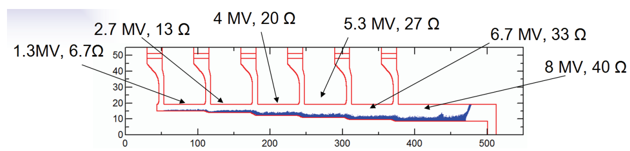

Figure. 6. Desired voltage and self-limited impedance in each section of the Mercury IVA on top of an LSP particle plot.

There are two MITL theories in common use are those originated by Creedon and Mendel. Although they have very different derivations, they deliver surprisingly similar results for the self-limited case. Creedon's theory is based on parapotential flow, where electrons move only in the axial direction within a flow layer of specified thickness from the cathode [9]. Mendel's theory does not specify the electron trajectories, but is based on the assumption of a uniform charge density within a specified thickness flow layer and a balance of magnetic and electric pressures within the flow [10].

Using Creeden theory, the equations to determine the required vacuum impedance, and hence center conductor diameter, in each of the six sections of MITL shown in Fig. 6 are

$$\begin{aligned}
\gamma_0 &= \frac{V_{MITL}}{511} + 1 \\
\gamma_0 &= \gamma_l + \left(\gamma_l^2 - 1\right)^{3/2} \ln\left(\gamma_l + \sqrt{\gamma_l^2 - 1}\right) \\
I_A &= \frac{511}{Z_{Vacuum}} \gamma_l^3 \ln\left(\gamma_l + \sqrt{\gamma_l^2 - 1}\right)
\end{aligned} \quad , \tag{2}$$

where Z_{Vacuum} is the vacuum impedance of the MITL to be calculated in Ω, V_{MITL} is the desired voltage in kV and I_A is the desired anode current (i.e., total current) in kA.

Using Mendel theory, which has been adjusted to fit LSP simulations by Ottinger [10], the relevant equations are

$$Z_f^{SL}(V) = Z_0 f_{SL}(V)$$

$$f_{SL}(V) = \eta \left\{ \frac{\left(\frac{gmc^2}{8eV} - 1\right) + \left[\left(\frac{gmc^2}{8eV} - 1\right)^2 + \left(\frac{gmc^2}{2eV} - 1\right)\right]^{1/2}}{\left(\frac{gmc^2}{2eV} - 1\right)} \right\}$$

$$\eta = 0.82 + 0.0086V$$

$$g = 0.99565 - 0.05332V + 0.0037V^2 \qquad (3)$$

where Z_0 is the vacuum impedance of the MITL to be calculated, Z_f^{SL} is the effective impedance of the MITL in Ω, V is the MITL voltage in MV, and mc^2/e is 0.511 MV.

There is a slight difference in the meaning of the Creeden and Mendel results. Creeden calculates the desired impedance through the desired voltage divided by desired total current, V/I_A, whereas Mendel calculates an effective, "flow impedance", of the line, Z_f. From the relationship between Z_f, voltage, and anode and cathode currents,

$$Z_f = \frac{V}{\left(I_A^2 - I_C^2\right)^{1/2}} \qquad (4)$$

it is clear that V/I_A will always be slightly less than Z_f. Normally, Z_f and V/I_A are close enough that this difference is not significant. However, it is interesting to note that the Mendel MITL running with a self-limited load is not perfectly matched to this load, as often assumed. A self-limited load is always slightly under matched to Z_f.

C. Using a Non-Ideal Center Conductor

To save significant amounts of time and money, several options were considered for reusing sections of the original center conductor. The ideal center conductor diameters for each section were calculated for the values shown in Fig. 6, using Creedon, Eq. (2), in this case, and tabulated in Table 1 (left). Although several other center conductor options were considered [11], this case has two section diameters that are identical to diameters from the existing 6-MV center conductor listed in Table 1 (right). The first section in the 8-MV center conductor was the second section of the 6-MV center conductor, athough it is not an exact match to the ideal diameter. So, the final design used old parts for the first three sections and new parts for the final three sections, as listed in Table 1 (center).

Ideal Center Conductor			8-MV Center Conductor			Existing Center Conductor		
#	Z_0	OD [in.]	#	Z_0	OD [in.]	#	Z_0	OD [in.]
1	10.8	12.53	1	14.1	11.85	1	8.25	13.07
2	18.9	10.94	2	18.9	10.94	2	14.1	11.85
3	26.7	9.62	3	26.7	9.61	3	18.9	10.94
4	34.2	8.48	4	34.2	8.48	4	22.9	10.24
5	41.7	7.49	5	41.7	7.49	5	26.7	9.61
6	49.0	6.63	6	49.0	6.63	6	30.0	9.09

Table 1. Ideal center conductor section diameters (left), 6-MV diameters (right), and chosen 8-MV diameters (center).

For additional savings, the three new sections were constructed of aluminum instead of the stainless steel like the original. It was decided that the smaller diameter of these sections reduced the weight enough to allow fabrication with aluminum. Also, most of the stress is on the first sections of center conductor, which are all still stainless. A drawing of the new conductor is shown in Fig. 7. The only other machining required was the shorting of an existing base section (near left end in Fig. 7) and a new tapered section between MITL sections 2 and 3.

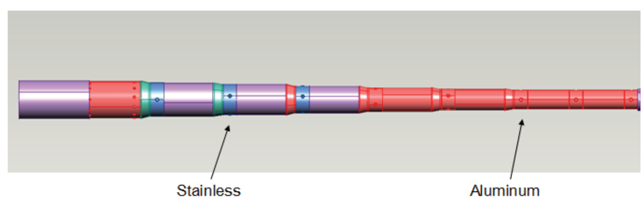

Figure 7. Drawing of the new 8 MV center conductor with new or modified parts shown in bright red.

Because the center conductor designs were non-ideal, LSP modeling was performed on several candidate designs to verify performance. Some designs considered earlier were ruled out because they did not equally balance the cell voltages and would cause one cell to be a weak link since the cells are now being stressed to the maximum design voltage.

Other designs caused excessive flow current because of a bad transition in the MITL. A bad transition occurs when the upstream electron flow section of MITL has a less than ideal impedance and/or the downstream section has a greater than ideal impedance. By Mendel theory, flow should be lost to the outer conductor at such a transition. But, LSP modeling shows that instead of flow being lost at a bad transition, it just adds to the flow current, although perhaps if our MITL were longer, it would be lost. Besides just an increase in flow current, the flow current becomes unstable with a bad transition and vortices in the flow current appear which lead to

oscillations in the load voltage and current. Both the increase in flow current and the oscillations can negatively influence the performance of diode loads. An example result of an LSP simulation of a bad center conductor design that produced unequal voltages and also oscillating, turbulent flow is shown in upper plot of Fig. 8. The lower plot in Fig. 8 shows the smooth flow produced with the center conductor of the final design.

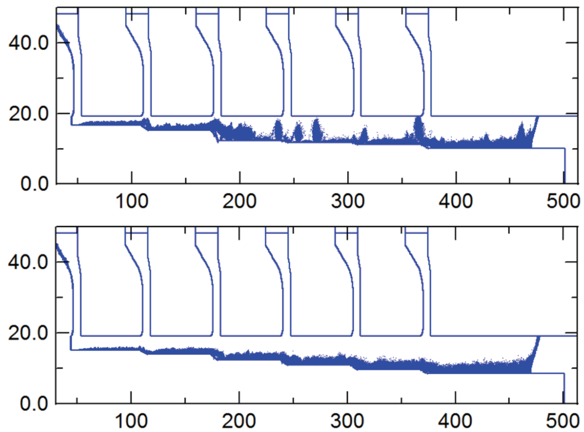

Figure 8. Example LSP particle plots of an inferior center conductor design (above) with turbulent flow and that of the final design (below)

Other designs were ruled out because they gave a load voltage greater than 8 MV at 75-kV charge. Because we needed to operate in the self-limited mode and 8 MV was considered the maximum safe operating voltage, we would have had to reduce the Marx charge voltage, which would have meant less diode current. Conversely, the final design also gave us the leeway to increase the Marx charge voltage up to 78-kV, where it has been operated in the past, in case it did not achieve 8.0 MV with 75 kV.

IV. MERCURY VOLTAGE LIMITATIONS AND PERFORMANCE

Mercury has now successfully fired over 200 shots with the new, 8-MV center conductor. However, there were initial concerns about if and for how long the cells could operate at 1.3 MV each.

A. Cell Voltage Limitations

The Mercury induction cells were designed to operate with 1.0 MV output but handle a 1.3 MV inductive spike at the cell insulator [12]. Our initial inspection of the Mercury cells revealed significant damage to the feedgap area between vacuum insulators and MITL due to arcing between 5-cm spaced faces. Fortunately, this problem was previously corrected by increasing the feedgap to 7-cm. Electrostatic field plots, like those shown in Fig. 9, were performed to verify that the insulators were still sharing the voltage just as equally. The conductor on the left side of Fig. 9 was moved left 2-cm in the feedgap area, where it was flat in the original design.

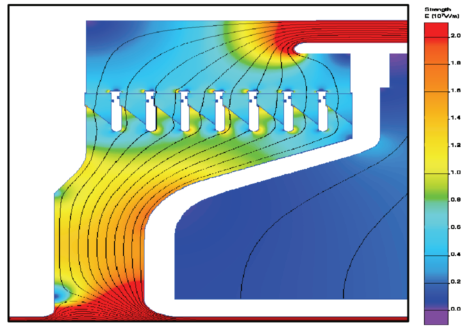

Figure 9. Electrostatic field plot of the feedgap and oil/vacuum barrier insulator of the Mercury cell.

One major concern was tracking of the oil/vacuum barrier insulators inside the cell. As shown in Fig. 9, this insulator is a segmented ring design with 8 insulators. The load voltage is reduced when a cell insulator stack fails, which can result in a bad shot. Several ring failures had occurred during the ~800 shots at 6-MV, which had on occasion led to oil leaking into the vacuum system and damaging the cryogenic vacuum pumps.

Another concern is increased stress on the magnetic cores (occupying the large blue area in Fig. 9). The cores consist of alternating metal and insulator windings and breakdown of this insulator is a concern with the higher voltage, which would lead to earlier saturation and a reduced pulse width. The cell cores are specified to have 65 mVs, but 8 MV for 50 ns divided by 6 cells equals 67 mVs, leaving very little margin.

One encouraging finding was that the previously mentioned inductive voltage overshoot at the insulators does not increase as one might expect. The length of the insulator stack has a large inherent inductance which reduces output risetime and causes the 1.3 MV voltage overshoot with 6 MV operation. Simulations show that with 8 MV output, this overshoot reduced. Also encouraging was that the cells have survived operation with 78-kV Marx charge with the old center conductor where the overshoot was about 1.4 MV.

B. Performance with New Center Conductor

The new center conductor has performed as expected, producing 8 MV output with 75-kV Marx charge. Prior to 75-kV shots, a series of shots were taken with 50-kV Marx charge and a variable impedance diode load. At the highest impedance, the MITL runs self-limited and the measured current and voltage were very near the intersection of the 50-kV load line and the new self-limited curve as shown in Fig. 10. Significant deviation from this simple load line is observed with lower

impedance loads, believed due to impedance mismatch in the adder under this condition.

Many shots at 75-kV Marx charge have been taken, all with a self-limited load. Data from the first seven shots is shown in Fig. 10 where, as expected, Mercury now runs at 8 MV and 200 kV with the new center conductor. After hundreds of shots, there have been several damaged insulator rings that had to be replaced. Because the failure rate is noticeably greater than at 6 MV, we have begun re-anodizing some damaged parts of the cell and acquiring Rexolite insulators to replace the current acrylic cell insulators.

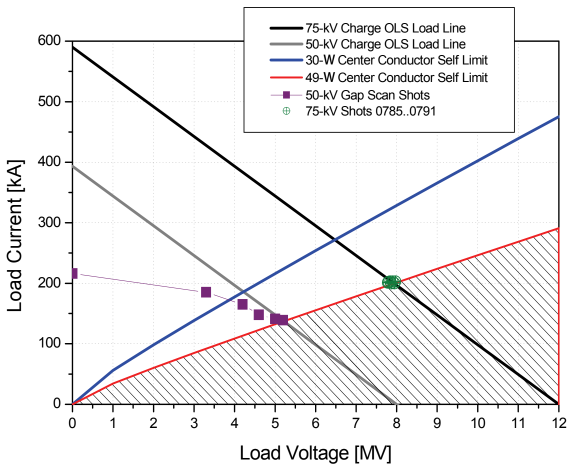

Figure 10. 75 and 50-kV Marx charge load lines with old and new self-limited impedance curves and measured data with variable load at 50 kV (purple squares) and self-limited load at 75 kV (green circles).

V. SUMMARY

The center conductor of Mercury has been replaced with a narrower version, allowing us to extend the operating point to 8 MV. As clearly shown with a load line, the output current is reduced from 300 to 200 kA with this change. But, because we are keeping the same 75-kV Marx charge voltage, we reduce the risk of damage to critical machine components such as IS, PFL, and laser switches that would have been stressed beyond design limits if we were to try reaching 8 MV by raising the Marx voltage.

To save time and money, several existing sections of center conductor were used, resulting in a non-ideal design. The final design was validated with LSP. Mercury has now had more than 200 successful shots at 8 MV.

VI. REFERENCES

[1] R.J. Allen, et al., “Initialization and operation of Mercury, a 6-MV MIVA,” 15th IEEE International Pulsed Power Conference, June 13-17 (2005).

[2] D.D. Hinshelwood, et al., “High-power, pulsed bremsstrahlung source for inducing photofission” these Proceedings.

[3] D.M. Mosher, et al., "A computation-based analysis of photon-induced fission," these Proceedings.

[4] J.P. Apruzese, et al., "Room scattering effects on the measured spatial distribution of delayed photofission neutrons from depleted uranium," 38th IEEE International Conf. on Plasma Sci., (Chicago, IL, June 2011).

[5] S.B. Swanekamp, et al., "An Analysis of Intense Pulsed Active Detection (IPAD) for the Detection of Special Nuclear Materials," *Nuclear Science, IEEE Transactions on* , 2011, to be published.

[6] V. L Bailey, et al., "Design of a High Impedance MITL for RITS-3", 14th IEEE Pulsed Power Conference proceedings, June 15-18 (2003), pp. 399-402.

[7] I.D. Smith, “Induction voltage adders and the induction accelerator family”, Phys. Rev. ST Accel. Beams 7, 064801 (2004)

[8] D.V. Rose, et al,, "Coupled particle-in-cell and Monte Carlo transport modeling of intense radiographic sources," J. Appl. Phys. **91**, 3328–3335 (2002).

[9] J.M. Creedon, “Magnetic cutoff in high-current diodes”, Appl. Phys. 48, 1070 (1977).

[10] P.F. Ottinger and J. W. Schumer, “Rescaling of equilibrium magnetically insulated flow theory based on results from particle-in-cell simulations”, Physics of Plasmas 13, 063109 (2006), and references therein.

[11] R.J. Allen, et al., “Circuit simulation of the MITL in an IVA with a non-ideal center conductor” 16th IEEE International Pulsed Power Conference, June 17-22 (2007).

[12] J. Fockler, “Design of a 6 MV, 2 TW positive ion driver using an induction adder”, 9th IEEE International Pulsed Power Conference, June 21-23 (1993)